

THE EFFECT OF IR IMPERFECTION ON DYNAMIC APERTURE IN SUPERKEKB/ DYNAMIC APERTURE STUDY OF CEPC

H. Sugimoto, KEK, Tsukuba, Japan

Abstract

Interaction region (IR) is the most critical part of colliders to optimize the dynamic aperture because a detector solenoid and strong final focus magnets give rise to complicated nonlinear beam dynamics. Design of the SuperKEKB IR has been carried out with considering the effect of a possible IR imperfection on the machine performance. In this paper, degradation of dynamic aperture due to error fields from the final focus magnets is discussed. We also present a preliminary study of dynamic aperture of CEPC based on the experience of the SuperKEKB lattice design.

INTRODUCTION

The KEKB accelerator [1] is being upgraded to a SuperB accelerator named SuperKEKB [2]. SuperKEKB consists of 7 GeV electron (HER) and 4 GeV positron (LER) storage rings with an injector linac and a positron damping ring. The target luminosity of $8 \times 10^{35} \text{ cm}^{-2} \text{ s}^{-1}$ is obtained by 2 times higher beam current (3.6 A for e^+ and 2.6 A for e^-), 1/20 times smaller vertical beta function β_y^* (0.3 mm), and larger crossing angle of 83 mrad. This approach also requires the low emittance optics to realize the nano-beam collision. The Touschek effect is enhanced in such a low emittance beam and restricts the beam lifetime. Meanwhile squeezing the beta function at the interaction point (IP) results the huge natural chromaticity and makes the chromaticity correction difficult. Furthermore the huge beta function enhances the undesired nonlinear effects in IR likely restricts the beam stability. Therefore the optimization of the dynamic aperture is one of the most challenging topic of the SuperKEKB lattice design.

A large number of feedback procedures between hardware and optics group have been repeated with consideration on detailed hardware specifications to obtain the sufficiently wide dynamic aperture. Overview of the lattice design and effects of the error fields due to the IR imperfection are reported in this paper.

Optimization of the dynamic aperture is a common issue on future high energy circular colliders. Sufficiently wide momentum acceptance is especially important requirement because the beamstrahlung is critical in such a high energy collider. We recently started the optimization of the dynamic aperture for the CEPC project proposed in China. In this paper, a preliminary study of the dynamic aperture of the CEPC lattice is also presented.

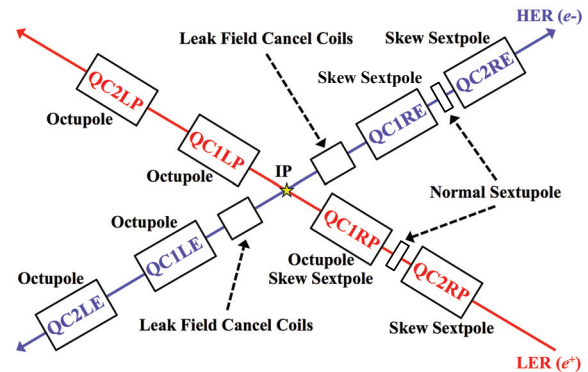


Figure 1: IR schematic view and arrangement of higher-order corrector coils. All magnets have superconducting corrector coils of a dipole, a skew dipole and a skew quadrupole.

SUPERKEKB IR DESIGN OVERVIEW

Figure 1 shows schematic view of the SuperKEKB IR [3]. Each storage ring has 4 superconducting magnets to squeeze the beam size at IP. All quadrupole magnets except for QC1Ps have iron or permendur yoke for preventing leakage fields to the opposite beam line. The HER beam line has cancel coils of sextuple, octupole, decapole and dodecapole in order to compensate the leakage field from QC1Ps of the LER beam line.

The SuperKEKB IR has a detector solenoid of 1.5 T, and this solenoid field is troublesome in the design of the beam optics and optimization of the dynamic aperture. For example, the finite crossing angle between the beam line and the solenoid axis generates the vertical emittance due to the solenoid fringe field. Therefore, the angle between solenoid axis and two beam lines should be chosen by compromising the vertical emittance generation in HER and LER. In the SuperKEKB IR design, this angle is chosen to be half of the crossing angle. Compensation solenoids are installed in order to suppress the effect of the solenoid field on the beam optics as much as possible. The field distribution is optimized so that the solenoid field integral from IP to each side of IR vanishes, $\int B_z(s) ds = 0$ for coupling matching, and reduce the peak of $\partial B_z / \partial s$ for vertical emittance suppression.

All quadrupole magnets have superconducting corrector coils of a dipole, a skew dipole and a skew quadrupole. Horizontal or vertical offset of the quadrupole magnets from the beam line is adopted to reduce required field strength of the dipole corrector in orbit matching. In addition to these

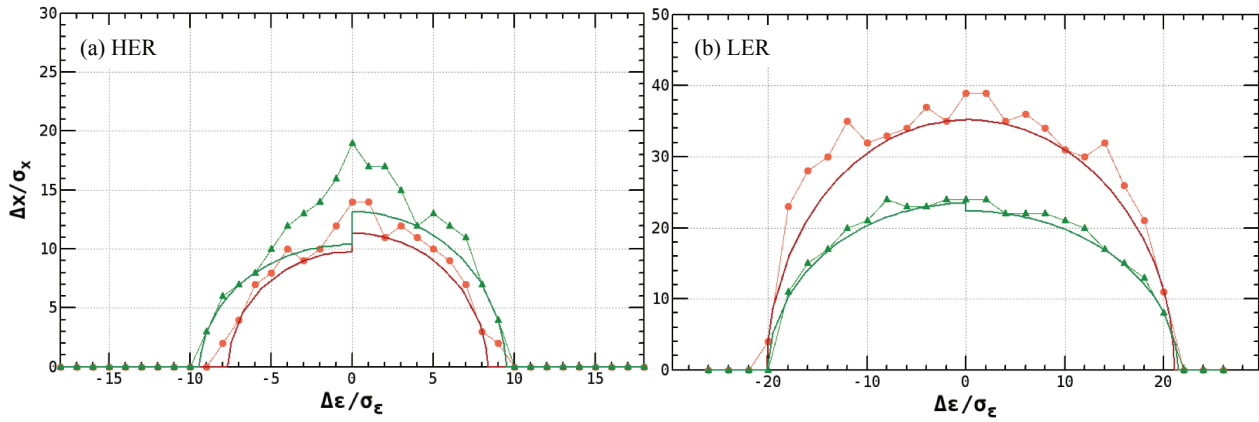


Figure 2: Dynamic aperture of (a) HER and (b) LER. Horizontal and vertical axes represent horizontal and momentum space in unit of their equilibrium values, respectively. The initial vertical amplitude of the tracking particle is chosen to be 0.27% of the initial horizontal amplitude. The initial horizontal and vertical betatron phases (ϕ_{x0}, ϕ_{y0}) are (0,0) (dots) and $(\pi/2, \pi/2)$ (triangles).

low order correctors, sextupole and octupole coils are installed to optimize the dynamic aperture. The arrangement of sextupole and octupole coils is determined by tolerance of QCS imperfections. Rotations of the quadrupole magnets are also introduced in LER to help the optics matching. Huge chromaticity originated in the extremely strong focusing in IR is compensated by the local chromaticity correction (LCC) scheme with sextupole magnets installed near IR.

The dynamic aperture is evaluated by particle tracking simulation using accelerator modeling code SAD [4]. Accurate modeling of IR is essential for reliable numerical simulation. In our approach, the full three-dimensional (3D) magnetic field is modeled by series of multiple slices. The multipole strengths are evaluated from multipole filed expansion of 3D field calculated by ANSYS code [5]. The multipole fields up to 44 poles are take into account, and the thickness of the multipole slice is chosen to be 1 cm. Figure 2 shows the dynamic aperture of LER and HER, where the dynamic aperture is evaluated through 1000-turn particle tracking simulation without beam-beam force, synchrotron radiation and quantum excitation.

We re-optimize the linear optics and dynamic aperture every time the IR hardware design is updated. Typical procedure for the re-optimization is briefly described as follows. We first evaluate the 3D field distribution using ANSYS code taking into account hardware design changes, then the IR model is updated by the multipole filed expansion of the 3D field data. After updating the IR model, orbit and linear optics matching is performed. Finally the dynamic aperture is optimized by the Down-hill simplex algorithm. Available knobs are 54 sextupole pairs along the ring and octupole correctors (3/LER, 2/HER) installed in IR. Finite amplitude matching and off-momentum optics matching are employed to find the initial set of the knob parameters as needed.

QCS IMPERFECTION

Field measurement of the QC1P prototype shows unexpected normal and skew sextupole field, and their field strength is $\sim 0.1\%$ of the main quadrupole field. These error fields are likely due to misalignment of the main coils of a few tens of μm . Numerical simulation study is conducted to investigate its effect on the dynamic aperture.

Figure 3 shows degradation of the LER dynamic aperture due to the error field, where Touschek lifetime evaluated by the dynamic aperture as a function of the amplitude of skew sextupole error field is plotted. For simplicity, the error field is modeled by thin sextupole lens attached to the beam line. In this simulation. We assume that only QC1LP and QC1RP magnets has error field, and their magnitudes are identical. All 4 possible combinations of signs of the sextupole field are evaluated in Fig. 3. The sextupole field

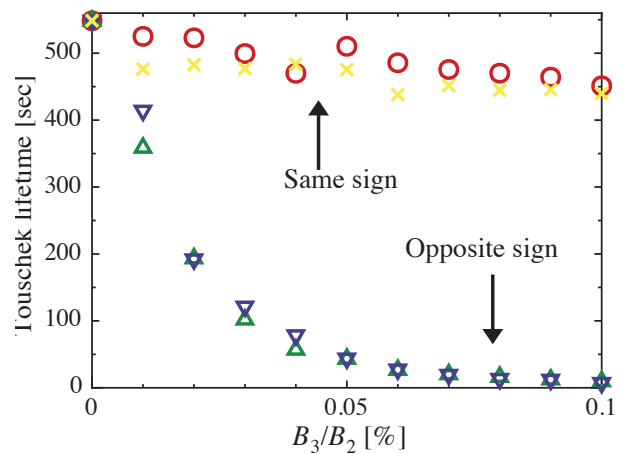


Figure 3: Touschek lifetime of LER as a function of the amplitude of skew sextupole error field, where horizontal axis indicates the ratio of skew sextupole field B_3 to quadrupole field B_2 .

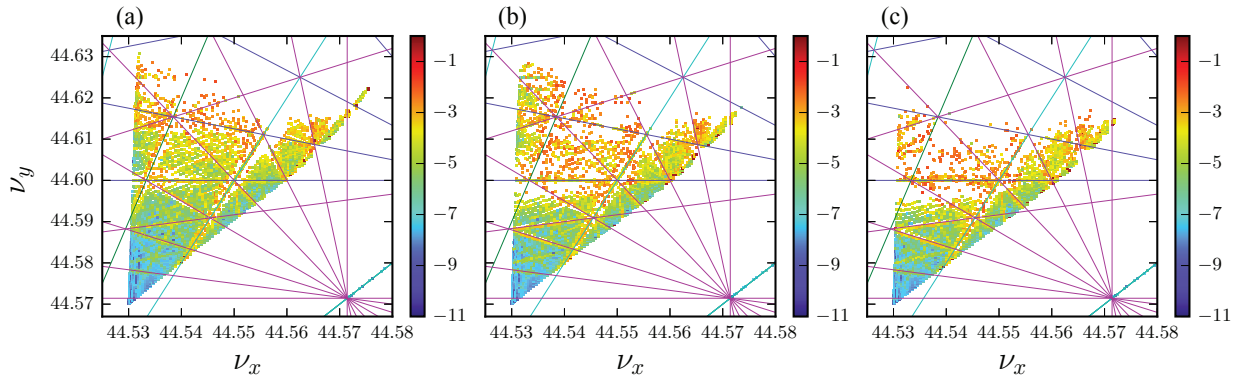


Figure 4: Footprints of LER with (a) $B_3/B_2 = 0$, (b) $5 \times 10^{-3}\%$, and (c) $1 \times 10^{-2}\%$.

reduces the dynamic aperture even though the error field is order of 0.01 % of the quadrupole field, B_2 . Since the betatron phase advance between QC1RP and QC1LP are almost π , the degradation of the dynamic aperture is less serious when their signs are same.

In order to reveal the effect of the error field in view point of the resonance instability, frequency map analysis [6] is applied. An illustrative result is shown in Fig. 4, where the so-called footprint of LER with three different error amplitude is plotted. The color indicates the tune diffusion rate defined by $\log_{10} \sqrt{(\nu_{x1} - \nu_{x2})^2 + (\nu_{y1} - \nu_{y2})^2}$, where ν_{x1} and ν_{y1} respectively denote the horizontal and vertical tunes calculated by the tracking data of first 1000 turns, ν_{x2} and ν_{y2} are those for the following 1000 turns. The NAFF algorithm [6], which is a more accurate technique compared to the fast Fourier transform is applied in the tune calculation. The tracking simulation is done for on-momentum particle without the synchrotron motion. We found that the sextupole error field excite the 5-th order resonances around $\nu_y = 44.6$. Taking these results, we decided to install the sextupole and skew sextupole coils to the final focus system (QCS) as show in Fig. 1.

Similar numerical simulations for higher order multipole error fields are also carried out to estimate the tolerance of the field quality of the QCS magnets. The simulation results are summarized in Fig. 5, where multipole error fields of $n = 4 \sim 10$ are evaluated individually. The multipole field of $n = 4$ here means decapole field. In the simulation, the thin lens multipoles are inserted to the all QCS magnets, and their magnitudes are identical. The worst case among the all 16 possible combinations of signs of the error field are plotted in Fig. 5. As expected, reduction of the dynamic aperture becomes smaller when n becomes larger. In the case of HER, the multipole of $n = 10$ is almost negligible at least in this parameter range. On the other hand, the multipole of $n = 10$ significantly reduces the dynamic aperture of LER even when B_n/B_2 is less than 0.01 %. In other word, LER is more sensitive to the nonlinear distortion compared with HER. Touschek effect is stronger in the LER owing to the lower beam energy. Thus, as shown in

Fig. 2, the particle with larger amplitude has to be stable in order to obtain the same Touschek lifetime as HER. These numerical results are now considered as the tolerance of the field quality of the QCS magnets.

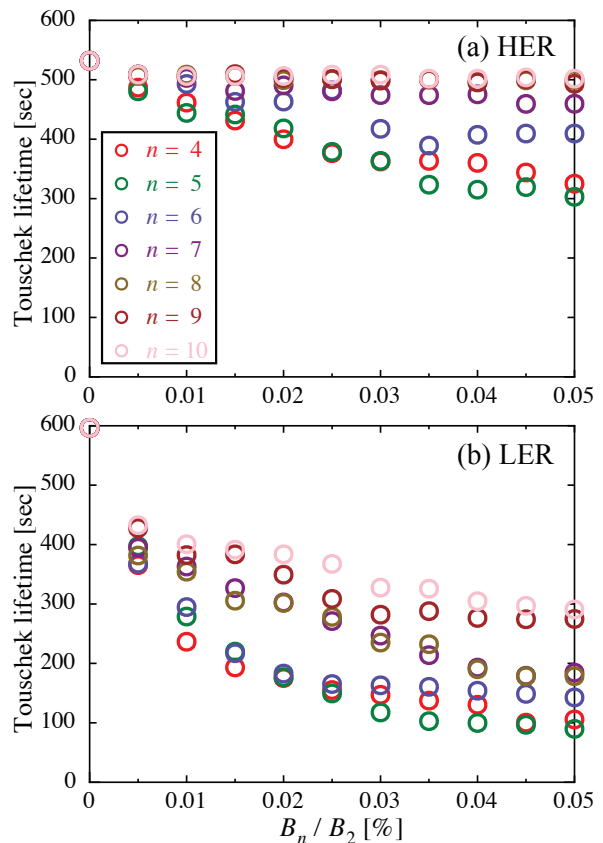


Figure 5: Touschek lifetime of (a) LER and (b) LER as a function of the amplitude of higher order multipole error fields.

CEPC LATTICE AND DYNAMIC APERTURE

CEPC is a large e^+e^- collider for a Higgs factory. The project is now under study to complete a preliminary conceptual design report (Pre-CDR) by the end of 2014. We recently started the study of the dynamic aperture of the CEPC lattice. The one of most challenging beam optics issue is the sufficiently wide momentum acceptance of $\pm 2\%$ for strong beamstrahlung effects. In the following parts of this paper, We present the first survey on the CEPC lattice and very preliminary study on the dynamic aperture based on the experience of the SuperKEKB lattice design.

Optics

Optical function in the arc lattice is shown in Fig. 6. The arc cell is based on a 60 degrees FODO cell. The sextupole magnets are installed next to each quadrupole for the chromaticity correction. Although the FODO cell is better for high packing factor, KEKB-type arc cell, a cell with non-interleaved sextupole pairs [7], is probably preferable in terms of optimization of the dynamic aperture since the required momentum acceptance of $\pm 2\%$ is very challenging. Possibility of applying other type of cell should be investigated in near future.

Figure. 7 shows the optical function in the final focus system (FFS). FFS is composed of the sections for horizontal and vertical local chromaticity corrections (X-LCC and Y-LCC) with $-I$ sextupole pairs. The betatron phase advance between sextupole is π to cancel the undesired nonlinear kick from the sextupoles. The vertical phase advance between final defocusing quadrupole (Q1FFS) and Y-LCC is π . On the other hand, the horizontal phase advance between the final focusing quadrupole (Q2FFS) and X-LCC is 3π . Changing this horizontal phase advance from 3π to 2π may improve the performance of the X-LCC, and it should be studied in near future.

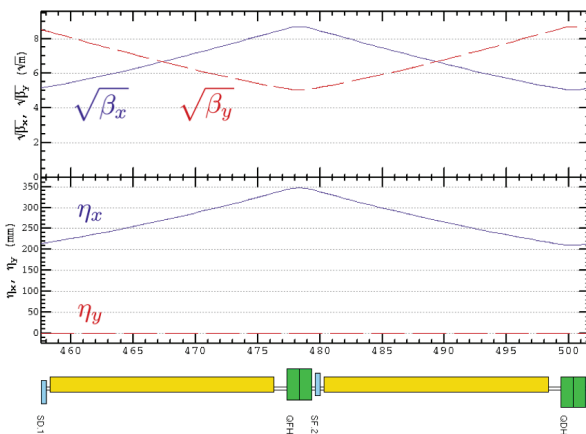


Figure 6: Optical functions of the CEPC arc cell.

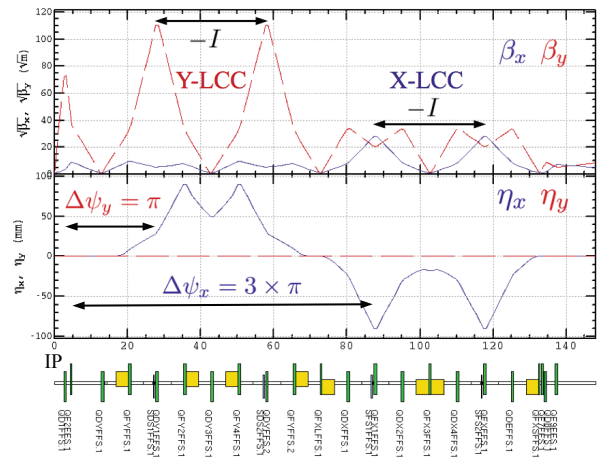


Figure 7: Optical functions in FFS.

Table 1: Natural Chromaticity (ξ_x, ξ_y)

	SuperKEKB HER	SuperKEKB LER	CEPC
FFS	(-108, -1022)	(-54, -721)	(-108, -2404)
Arc	(-38, -29)	(-31, -33)	(-182, -188)
Others	(-23, -19)	(-19, -35)	(-31, -25)
Total	(-169, -1070)	(-104, -789)	(-321, -2617)

Lattice Nonlinearity

The natural chromaticity of CEPC lattice is shown in Table 1 with comparison to that of SuperKEKB. As usual, FFS is the most dominant source of the natural chromaticity. Total natural chromaticity is more than twice as large as that of SuperKEKB. The essential difference between SuperKEKB and CEPC is number of IPs. The CEPC lattice has 2 IPs. The chromaticity correction, therefore, is probably more difficult than SuperKEKB.

It is well known that the nonlinearity around IP restricts the dynamic aperture. The dynamic aperture associated to the both the kinematic term and nonlinear fringe of the final focus magnet is given by [7],

$$J_{y0} = \frac{\beta_y^{*2}}{(1 - 2k_1 l^{*2}/3) l^*} A(\mu_y), \tag{1}$$

where J_{y0} is aperture for the original action, the β_y^* is the vertical beta function at IP, l^* is the distance between IP and the quadrupole face, and k_1 is the focusing strength. The function $A(\mu_y)$ is a universal function which depends only on the fractional part of the vertical tune [4], thus the ratio between $J_{y0}/A(\mu_y)$ gives us an index of the dynamic aperture associated to the nonlinear terms around IP. Table 2 shows these parameters of CEPC lattice with comparison to those of KEKB and SuperKEKB. The ratio $J_{y0}/A(\mu_y)$ of CEPC is similar order of magnitude to that of SuperKEKB.

Table 2: Nonlinear Terms Around IP

	SuperKEKB		SuperKEKB	CEPC	Units
	KEKB	HER	LER		
β_y^*	5900	300	270	1200	μm
k_1	-1778	-3.0539	-5.104	-1.2881	$1/\text{m}^2$
l^*	1.762	1.221	0.766	2.5	m
$J_{y0}/A(\mu_y)$	4.22	0.0183	0.0317	0.0904	μm

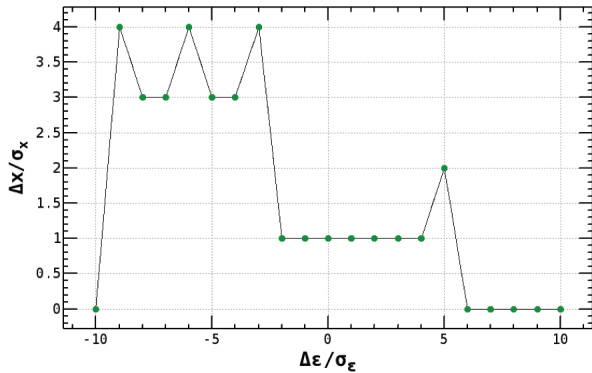


Figure 8: Dynamic aperture of the presented CEPC lattice. Horizontal and vertical axes represent horizontal and momentum space in unit of their equilibrium values, respectively. The initial vertical amplitude of the tracking particle is chosen to be 0.3% of the initial horizontal amplitude. The initial horizontal and vertical betatron phases (ϕ_{x0}, ϕ_{y0}) are (0,0).

Dynamic Aperture

The dynamic aperture of the presented CEPC lattice is shown in Fig. 8. The dynamic aperture is evaluated through 1000-turn particle tracking simulation. Even for on-momentum, dynamic aperture is far from the target values of $40\sigma_x$.

In order to investigate the dominant cause of the restriction of on-momentum dynamic aperture, we calculate on-momentum dynamic aperture with four different sextupole conditions. The sextupole conditions are listed in Table 3. In the all simulation, the synchrotron motion is frozen out to focus on the on-momentum beam dynamics. Simulation results are summarized Fig. 9(red bar). The result of case B shows the dynamic aperture is not improved by turning off the arc sextupole. The dynamic aperture is improved in some degree by turning off the sextupoles used in the LCC section (case C). According to these numerical results, we conclude that the geometric terms originated from the sextupole magnets seem to be too large in the presented CEPC lattice.

In addition to these simulation, we tried analogous simulations by turning off the fringe field of the final quadrupole magnets (blue bar). We notice that the fringe effect is not visible in case A, B, and C, while the dynamic aperture is remarkably improved in case D. The result indicates that

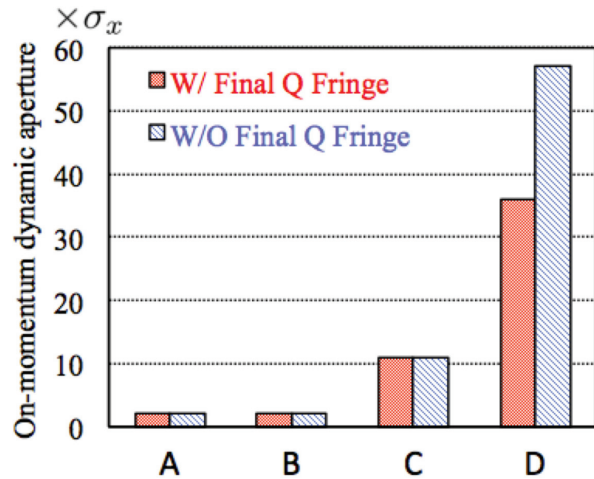


Figure 9: On-momentum dynamic aperture of the CEPC lattice with four different sextupole conditions. The sextupole conditions are listed in Table 3.

Table 3: Sextupole Conditions Assumed in Fig. 9

Case	Arc Sextupole	LCC Sextupole
A	On	On
B	Off	On
C	On	Off
D	Off	Off

the fringe effect will be important once the geometric term of the sextupole is minimized. In such cases some octupole correctors can be used to compensate the fringe effect because a quadrupole fringe field induces an octupole-like transverse kick.

On-momentum dynamic aperture as a function of the LCC sextupole strength is shown in Fig. 10. Figure. 10 says that the sextupole field is too strong for the required dynamic aperture of $40\sigma_x$. The Y-LCC sextupole should be reduced by about one-tenth. In order to reduce the sextupole strength, the horizontal dispersion function at the LCC sextupole magnets should be increased. However, the large dispersion function involves emittance generation and detector background due to the synchrotron radiation. Further study is, therefore, needed to optimize the FFS optics.

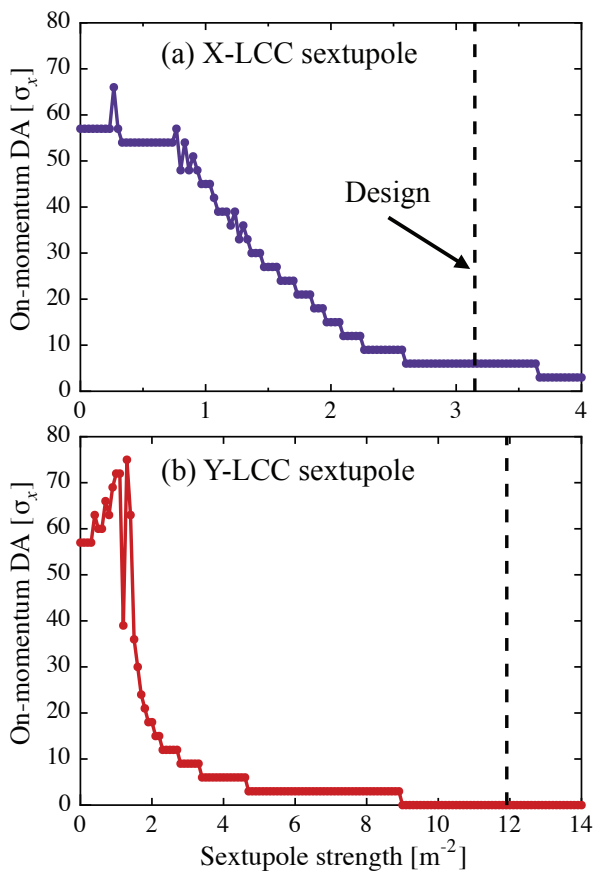


Figure 10: On-momentum dynamic aperture as a function of the (a) X-LCC sextupole and (b) Y-LCC sextupole strengths.

SUMMARY

The overview of the SuperKEKB IR design is presented. The effects of sextupole error field from QCS on the dynamic aperture is evaluated, and we decided to install normal and skew corrector coils to IR. We also present the tolerance of field quality of the final focus magnets by evaluating the effects of higher order multipole error field on the dynamic aperture.

A preliminary study on the dynamic aperture of the CEPC lattice is also reported. The dominant cause of the restriction of the dynamic aperture is the huge geometric terms originated from the LCC sextupole magnets. In order to decrease the sextupole strength, the horizontal dispersion at the LCC sextupole magnets should be increased. Further systematic study on the FFS optics is needed to improve the dynamic aperture.

ACKNOWLEDGEMENTS

The presented design study of the SuperKEKB IR is carried out by the SuperKEKB optics group. The author would like to thank the IHEP beam optics group for providing the information of CEPC lattice. The author also thanks A.

ISBN 978-3-95450-172-4

Morita and Y. Ohnishi for useful comments on the dynamic aperture study of CEPC.

REFERENCES

- [1] "KEKB B-Factor Design Report", KEK Report 95-7 (1995).
- [2] Y. Ohnishi *et al.*, Prog. Theor. Exp. Phys. 2013 03A011 (2013).
- [3] N. Ohuchi *et al.*, Proc. of PAC2013, Pasadena, USA, WEODA1, p.761 (2013).
- [4] K. Oide, Nucl. Inst. Meth. A **276**, 427 (1989). <http://acc-physics.kek.jp/SAD/>
- [5] ANSYS, <http://www.ansys.com>
- [6] L. Nadolski and J. Laskar, Phys. Rev. ST Accel. Beams **6**, 114801 (2003).
- [7] K. Oide and H. Koiso, Phys. Rev. E **47**, 2010 (1993).